Available online at www.sciencedirect.com
ScienceDirect
Journal of Sound and Vibration 297 (2006) 761–773
JOURNAL OF SOUND AND VIBRATION
www.elsevier.com/locate/jsvi

Acoustic analysis of elliptical muffler chamber having a perforated pipe

Nishimura Sohei[a,*], Nishimura Tsuyoshi[b], Yano Takashi[a]

[a]*Faculty of Engineering, Kumamoto University, 2-39-1 Kurokami Kumamoto, Japan*
[b]*Faculty of Computer Science, Sojo University, 4-22-1 Ikeda Kumamoto, Japan*

Received 30 December 2005; received in revised form 10 April 2006; accepted 21 April 2006
Available online 18 July 2006

Abstract

Evidently, a perforated pipe is an essential component in muffler systems. It has the ability to reduce the power levels of noise sources generated by flow. Muffler systems are composed of several elements joined together in series or parallel. In practical approach, each element can have one or more perforated pipe installed. This yields the ability to estimate the acoustic characteristic by the product of the individual element four-pole parameters.

In this work, a method to derive the four-pole parameters of such element with consideration of higher-order mode is presented. Based on the results obtained, the parameter C was investigated systematically. Some comparisons between the experimental measurements and the predicted results are discussed. The mean flow velocity is not considered in this paper.
© 2006 Elsevier Ltd. All rights reserved.

1. Introduction

Perforated pipes are a commonly used feature in muffler designs, mainly because of their ability to reduce the acoustic power of the noise generated by flow significantly influenced by its velocity [1–5]. Contemporary automotive muffler chambers consist of more than one resonance room and expansion room joined together in series, in which one or several perforated pipes are installed. In this case, the acoustic characteristics of mufflers can be easily estimated by obtaining the product of the individual element four-pole parameters. When the dimension of each element is small compared with the acoustic wavelength, the one-dimensional model four-pole parameter is frequently used. However, by the presence of a perforated pipe, the one-dimension frequency range will become extremely narrow due to the generation of higher-order modes at low-frequency range. In order to estimate the performance of mufflers in wide frequency range, the modeling or analysis of such an arrangement would require the expression of four-pole parameters including the higher order modes effect.

In the present work, a method to derive the four-pole parameters of an elliptical muffler chamber having a perforated pipe with the higher order mode effect is suggested. Perforated tube muffler is modeled as a

*Corresponding author. Tel.: +81 96 326 3978.
E-mail addresses: sohei0627@msn.com (N. Sohei), nisimura@cis.sojo-u.ac.jp (N. Tsuyoshi), yano@gpo.kumamoto-u.ac.jp (Y. Takashi).

0022-460X/$ - see front matter © 2006 Elsevier Ltd. All rights reserved.
doi:10.1016/j.jsv.2006.04.026

piston-driven rigid tube. The four-pole parameters are defined from the average sound pressure of the input and output piston, which are obtained by using the impedance model of perforated pipe. Based on the results obtained, the parameter C is investigated systematically. Some comparisons between the experimental measurements and the predicted results are also discussed. The mean flow velocity is not considered in this paper.

2. Analysis method

2.1. Model of analysis and boundary conditions

Consider the elliptic cylindrical cavity of eccentricity e_w and length l having a thin perforated pipe in elliptical form as shown in Fig. 1. The eccentricity of the input, of perforated pipe and of output are e_0, e_p and e_l, respectively. Assume that the acoustic impedance of perforated pipe can be regarded as uniform over its surface.

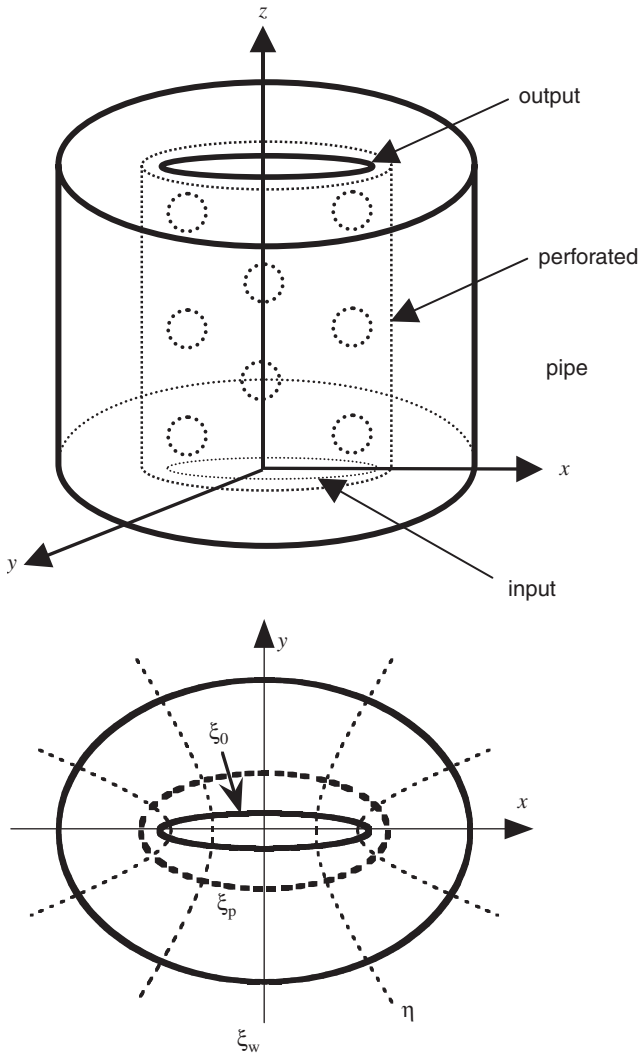

Fig. 1. Cross section and geometry of the problem.

The general solution of the wave equation in elliptical coordinates is a combination of some function as follows [6]:

$$\phi(\xi,\eta,z) = (A_0\ \exp(\mu z) + B_0 \exp(-\mu z))\left(\sum_{m=0}^{\infty} C_m Ce_m(\xi,s)ce_m(\eta,s) + \sum_{m=0}^{\infty} S_{m+1} Se_{m+1}(\xi,s)se_{m+1}(\eta,s)\right), \quad (1)$$

where $\phi(\xi,\eta,z)$ is the velocity potential, A_0, B_0, C_m and S_{m+1} are arbitrary constants determinable from the boundary conditions. Functions $ce_m(\eta,s)$ and $Ce_m(\xi,s)$ are even and even modified Mathieu function of mth order, respectively; $se_m(\eta,s)$ and $Se_m(\xi,s)$ are odd and odd modified Mathieu function of mth order, respectively. The value of s is defined by the following equation:

$$s = \frac{q^2}{4}(k^2 + \mu^2), \quad (2)$$

where q is the distance between the foci and the origin, $k = \omega/c$ with ω and c are the angular frequency and the sound velocity, respectively, μ is arbitrary constant.

Let the velocity potential inside the perforated tube be ϕ_{in} and that outside the tube be ϕ_{out}, respectively. Since the distribution of ϕ_{in} is symmetric about the major and the minor axis, ϕ_{in} must be even and periodic in η, hence the general solution of ϕ_{in} becomes

$$\phi_{\text{in}} = (A_i\ \exp(\mu z) + B_i\ \exp(-\mu z))\sum_{m=0}^{\infty} C_m Ce_m(\xi,s)ce_m(\eta,s). \quad (3)$$

Since ϕ_{out} has both symmetrical and unsymmetrical terms, the general solution of ϕ_{out} becomes

$$\phi_{\text{out}} = (A_0\ \exp(\mu z) + B_0\ \exp(-\mu z))\left(\sum_{m=0}^{\infty} C_m Ce_m(\xi,s)ce_m(\eta,s) + \sum_{m=0}^{\infty} S_{m+1} Se_{m+1}(\xi,s)se_m(\eta,s)\right). \quad (4)$$

The boundary conditions are as follows:

$$[1] \quad \text{at} \quad z = 0, \quad V_z = -\frac{\partial \phi_{\text{in}}}{\partial z} = V_0 F_0(\xi,\eta), \quad (5)$$

$$[2] \quad \text{at} \quad z = 1, \quad V_z = -\frac{\partial \phi_{\text{in}}}{\partial z} = V_l F_l(\xi,\eta), \quad (6)$$

$$[3] \quad \text{at} \quad \xi = \xi_w, \quad V_\xi = -\partial\phi_{\text{out}}/\partial\xi = 0, \quad (7)$$

$$[4] \quad \text{at} \quad z = l, \quad V_z = -\partial\phi_{\text{out}}/\partial z = 0, \quad (8)$$

where V_z and V_ξ are the velocity components in the z, and ξ directions, respectively, V_0 and V_l are the driving velocity at the input and the output piston, respectively, $F(\xi,\eta) = 1$ at the piston and $F(\xi,\eta) = 0$ elsewhere.

Let the sound pressure and the volume velocity inside the perforated pipe be P_{in} and U_{in}, respectively. Let those outside the perforated pipe be P_{out} and U_{out}, respectively. Then at the surface of perforated pipe $\xi = \xi_p$, the following relations are obtained:

$$P_{\text{in}} = P_{\text{out}} + Z_{\text{pipe}} U_{\text{out}}, \quad (9)$$

$$U_{\text{in}} = U_{\text{out}}, \quad (10)$$

where z_{pipe} is the impedance of perforated pipe. Since the sound pressure P and volume velocity U are related to the velocity potential ϕ by $P = \mathrm{j}k\rho c\phi$ and $U = \partial\phi/\partial\xi$, Eqs. (6) and (7) are then represented as

$$[5] \quad \text{at} \quad \xi = \xi_p, \quad \phi_{\text{in}} - \phi_{\text{out}} = \frac{Z_{\text{pipe}}}{jk\rho c}\frac{\partial\phi_{\text{out}}}{\partial\xi}, \quad (11)$$

$$[6] \quad \text{at} \quad \xi = \xi_p, \quad \partial\phi_{\text{in}}/\partial\xi = \partial\phi_{\text{out}}/\partial\xi. \quad (12)$$

2.2. Sound pressure on the input and output piston

According to the above boundary conditions, ϕ_{in} can be determined (see Appendix A). Therefore, the sound pressure at the input piston of the chamber corresponding to ϕ_{in} becomes

$$P_0 = \mathrm{j}k\rho c\,\phi_{\text{in}}|_{z=0} = \mathrm{j}kZ_w \sum_{m=0}^{\infty}\sum_{i=0}^{\infty}\Big(GT_{m,i}Q^0_{m,i}U_0 - GS_{m,i}Q^l_{m,i}U_l\Big)(1+\ddot{Z}_{m,i})\Theta_m(\xi,\eta,s_{m,i}), \tag{13}$$

where

$$GS_{m,i} = \frac{1}{\mu_{m,i}\sinh\,\mu_{m,i}l + \ddot{Z}_{m,i}\overline{\mu_{m+1,i}}\sinh\overline{\mu_{m+1,i}}l}, \tag{14}$$

$$GT_{m,i} = \frac{1}{\mu_{m,i}\tanh\,\mu_{m,i}l + \ddot{Z}_{m,i}\overline{\mu_{m+1,i}}\tanh\overline{\mu_{m+1,i}}l}, \tag{15}$$

$$\mu_{m,i} = \frac{1}{a_w}\sqrt{\lambda^2_{m,i} - (ka_w)^2}, \tag{16}$$

$$\overline{\mu_{m+1,i}} = \frac{1}{a_w}\sqrt{\overline{\lambda^2_{m+1,i}} - (ka_w)^2}, \tag{17}$$

$$\lambda_{m,i} = 2\sqrt{s_{m,i}}/e_w, \tag{18}$$

$$\overline{\lambda_{m+1,i}} = 2\sqrt{\overline{s_{m+1,i}}}/e_w, \tag{19}$$

$$\Theta_m(\xi,\eta,s_{m,i}) = Ce_m(\xi,s_{m,i})ce_m(\eta,s_{m,i}), \tag{20}$$

$$Q^u_{m,i} = \frac{S_w}{S_0}\int_0^{\xi_u}\int_0^{2\pi}\Theta_m(\xi,\eta,s_{m,i})g(\xi,\eta)\mathrm{d}\xi\mathrm{d}\eta \Big/ \int_0^{\xi_w}\int_0^{2\pi}\Theta^2_m(\xi,\eta,s_{m,i})g(\xi,\eta)\mathrm{d}\xi\mathrm{d}\eta, \tag{21}$$

$$g(\xi,\eta) = \cosh 2\xi - \cos 2\eta. \tag{22}$$

$U_0 = V_0S_0$ and $U_l = V_lS_l$ are volume velocity at input and output, respectively, S_0, S_l and S_w are cross-sectional area of input, output and chamber, respectively, $Z_w = \rho c/S_w$, a_w is major semi-axis of elliptical chamber, $\ddot{Z}_{m,i}$ is given in Eq. (A.24) (see Appendix A), the term related to the acoustic impedance of perforated pipe.

Similarly, the sound pressure on the output side ($z = 1$) is given by

$$P_l = \mathrm{j}k\rho c\phi_{\text{in}}|_{z=1} = \mathrm{j}kZ_w\sum_{m=0}^{\infty}\sum_{i=0}^{\infty}(GS_{m,i}Q^0_{m,i}U_0 - GT_{m,i}Q^l_{m,i}U_l)(1+\ddot{Z}_{m,i})\Theta_m(\xi,\eta,s_{m,i}). \tag{23}$$

2.3. The average sound pressure on input and output piston

Let $\mathrm{d}s_1\mathrm{d}s_2$ be an elemental cross-sectional area as shown in Fig. 2 with

$$\begin{aligned}\mathrm{d}s_1\mathrm{d}s_2 &= [(\delta x/\delta\xi)^2 + (\delta y/\delta\xi)^2]d\xi[(\delta x/\delta\eta)^2 \\ &\quad + (\delta y/\delta\eta)^2]\mathrm{d}\eta = \frac{q^2}{2}(\cosh\,2\xi - \cos\,2\eta)\mathrm{d}\xi\mathrm{d}\eta.\end{aligned} \tag{24}$$

Then the average sound pressure acting on the output piston can be expressed as

$$\overline{P_0} = \frac{1}{S_0}\int_0^{\xi_0}\int_0^{2\pi}P_0\mathrm{d}s_1\mathrm{d}s_2 = jkZ_w\sum_{m=0}^{\infty}\sum_{i=0}^{\infty}\Big(GT_{m,i}\overline{Q^{0,0}_{m,i}}U_0 - GS_{m,i}\overline{Q^{0,l}_{m,i}}U_l\Big)(1+\ddot{Z}_{m,i}), \tag{25}$$

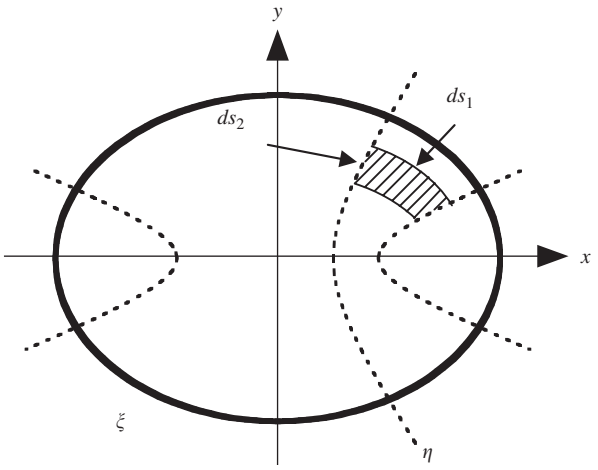

Fig. 2. Elemental area on the input and output piston.

where

$$\overline{Q_{m,i}^{u,v}} = \frac{q^2}{2}\frac{S_w}{S_u S_v}\frac{\int_0^{\xi_u}\int_0^{2\pi}\Theta_m(\xi,\eta,s_{m,i})g(\xi,\eta)\mathrm{d}\xi\mathrm{d}\eta}{\int_0^{\xi_w}\int_0^{2\pi}\Theta_m^2(\xi,\eta,s_{m,i})g(\xi,\eta)\mathrm{d}\xi\mathrm{d}\eta}\int_0^{\xi_v}\int_0^{2\pi}\Theta_m(\xi,\eta,s_{m,i})g(\xi,\eta)\mathrm{d}\xi\mathrm{d}\eta. \tag{26}$$

Symbols u and v are 0 or l, respectively. Similarly, the average sound pressure on the output piston can be simplified as

$$\overline{P_l} = jkZ_w\sum_{m=0}^{\infty}\sum_{i=0}^{\infty}\left(GS_{m,i}\overline{Q_{m,i}^{0,l}}U_0 - GT_{m,i}\overline{Q_{m,i}^{l,l}}U_l\right)(1+\ddot{Z}_{m,i}). \tag{27}$$

2.4. The four-pole parameters

By setting $U_l = 0$ in Eqs. (25) and (27), the parameter A and C can be obtained as

$$A = \left.\frac{\overline{P_0}}{\overline{P_l}}\right|_{U_l=0} = \frac{\sum_{m=0}^{\infty}\sum_{i=0}^{\infty}GT_{m,i}\overline{Q_{m,i}^{0,0}}(1+\ddot{Z}_{m,i})}{\sum_{m=0}^{\infty}\sum_{i=0}^{\infty}GS_{m,i}\overline{Q_{m,i}^{0,l}}(1+\ddot{Z}_{m,i})}, \tag{28}$$

$$C = \left.\frac{U_0}{\overline{P_l}}\right|_{U_l=0} = \frac{1}{\mathrm{j}kZ_w\sum_{m=0}^{\infty}\sum_{i=0}^{\infty}GS_{m,i}\overline{Q_{m,i}^{0,l}}(1+\ddot{Z}_{m,i})}. \tag{29}$$

Next, by setting $P_l = 0$ in Eq. (27), we have the relationship between U_0 and U_l. Thus the parameter D and B can be obtained as

$$B = \left.\frac{\overline{P_0}}{\overline{U_l}}\right|_{\overline{P_l}=0} = \mathrm{j}kZ_w\sum_{m=0}^{\infty}\sum_{i=0}^{\infty}GS_{m,i}\left(\frac{GT_{m,i}^2\overline{Q_{m,i}^{0,0}}\,\overline{Q_{m,i}^{l,l}}}{GS_{m,i}^2\overline{Q_{m,i}^{0,l}}} - 1\right)\overline{Q_{m,i}^{0,l}}(1+\ddot{Z}_{m,i}), \tag{30}$$

$$D = \left.\frac{U_0}{U_l}\right|_{\overline{P_l}=0} = \frac{\sum_{m=0}^{\infty}\sum_{i=0}^{\infty}GT_{m,i}\overline{Q_{m,i}^{l,l}}}{\sum_{m=0}^{\infty}\sum_{i=0}^{\infty}GS_{m,i}\overline{Q_{m,i}^{0,l}}}. \tag{31}$$

Moreover, expanding the above parameters with mode (0, 0) and rewriting k by $k-\mathrm{j}\alpha$ in order to consider the attenuation constant α in the chamber, we have

$$A = \cosh(\alpha+\mathrm{j}k)l + \frac{\dot{\Sigma}\,GT_{m,i}\overline{Q_{m,i}^{0,0}}(1+\ddot{Z}_{m,i})}{\dot{\Sigma}\,GS_{m,i}\overline{Q_{m,i}^{0,l}}(1+\ddot{Z}_{m,i})}, \tag{32}$$

$$B = Z_w \sinh(\alpha + \mathrm{j}k)l + \mathrm{j}(k\mathrm{j} - \alpha)Z_w \dot{\Sigma} GS_{m,i} \left(\frac{GT_{m,i}^2 \overline{Q_{m,i}^{0,0}}\, \overline{Q_{m,i}^{l,l}}}{GS_{m,i}^2 \overline{Q_{m,i}^{0,l}}} - 1 \right) \overline{Q_{m,i}^{0,l}} (1 + \ddot{Z}_{m,i}), \tag{33}$$

$$C = 1 \Big/ \left(\frac{Z_w}{\sinh(\alpha + \mathrm{j}k)l} + (\mathrm{j}k + \alpha) Z_w \dot{\Sigma} GS_{m,i} \overline{Q_{m,i}^{0,l}} (1 + \ddot{Z}_{m,i}) \right), \tag{34}$$

$$D = \cosh(\alpha + \mathrm{j}k)l + \frac{\dot{\Sigma} GT_{m,i} \overline{Q_{m,i}^{l,l}}}{\dot{\Sigma} GS_{m,i} \overline{Q_{m,i}^{0,l}}}, \tag{35}$$

where the symbol $\dot{\Sigma}$ means $\sum_{m=0}^{\infty} \sum_{i=0}^{\infty}$ without $m = i = 0$.

3. Results and discussion

Four-pole parameters are derived from Eqs. (32)–(35) in which the first term represents the plane wave and the second, the transverse wave. Hereafter, in order to validate the previous theoretical developments, we consider the case of parameter C as shown by Eq. (34).

The calculated result of parameter C is shown by the solid line in Fig. 3(a), when we represent Eq. (34) in dB as

$$20 \,\mathrm{Log}_{10}|C| = 20 \,\mathrm{Log}_{10} \left| \frac{Z_w}{\sinh(\alpha + \mathrm{j}k)l} + (\mathrm{j}k + \alpha) \times Z_w \dot{\Sigma} GS_{m,i} \bar{Q}_{m,i}^{0,l} (1 + \tilde{Z}_{m,i}) \right|. \tag{36}$$

The parameter C will have a lower level corresponding to the frequencies at which these denominators $\sinh(\alpha+\mathrm{j}k)l$ and $\mu_{m,i} \sinh \mu_{m,i} l + \ddot{Z}_{m,i} \overline{\mu_{m+1,i}} \sinh \overline{\mu_{m+1,i}} l$ of $GS_{m,i}$ in Eq. (36) are zero. Namely, when $\sinh(\alpha + \mathrm{j}k)l = 0$, these frequencies are

$$f = n \frac{c}{2l} \quad (n = 0, 1, 2, \ldots). \tag{37}$$

For the second denominator $\mu_{m,i} \sinh \mu_{m,i} l + \ddot{Z}_{m,i} \overline{\mu_{m+1,i}} \sinh \overline{\mu_{m+1,i}} l$, it is difficult to find these frequencies when this denominator become zero logically. However, when $\ddot{Z}_{m,i}$, the term related to the acoustic impedance of the perforated pipe as defined by Eq. (A.34) in Appendix A, is extremely small, these frequencies can be found:

$$\mu_{m,i} \sinh \mu_{m,i} l = 0 \quad \therefore \quad f_{m,i}^{(1)} = \frac{c}{2\pi a_w} \sqrt{\lambda_{m,i}^2 + (n\pi a_w / l)^2}. \tag{38}$$

Oppositely, when $\ddot{Z}_{m,i}$ is very large, these frequencies become

$$\overline{\mu_{m+1,i}} \sinh \overline{\mu_{m+1,i}} l = 0 \quad \therefore \quad f_{m,i}^{(2)} = \frac{c}{2\pi a_w} \sqrt{\overline{\lambda_{m+1,i}^2} + (n\pi a_w / l)^2}, \tag{39}$$

where the relations of $\lambda_{m,i}$ and $\overline{\lambda_{m,i}}$ with the chamber eccentricity are shown in Fig. 4. Therefore, the frequencies where $\mu_{m,i} \sinh \mu_{m,i} l + \ddot{Z}_{m,i} \overline{\mu_{m+1,i}} \sinh \overline{\mu_{m+1,i}} l = 0$ appear between $f_{m,i}{}^{(1)}$ and $f_{m,i}{}^{(2)}$. The generation mechanism of these frequencies can be understood according to the calculation example shown in Fig. 3(b). The values of $\sin kl$ in Fig. 3(b) are shown on a magnification of $10\times$ for convenience.

From Fig. 3(a), it is observed that the lower level of mode (1,0) does not appear in the frequency range over 1750 Hz despite the fact that their denominator has zero values shown in Fig. 3(b). This is conceivable if the level of (1,0) is less than the one of mode (2,0), which has a first resonance at 1600 Hz and its level suddenly increases in the upper frequency range. This relationship is obvious from the calculated results, shown in Fig. 3(c) with a dotted line and solid line represents the computed results shown in Fig. 3(a) and mode (1,0) itself.

Our computations have been achieved with the attenuation factor α given by [7]

$$\alpha = 0.02203 \sqrt{\frac{f}{2cr_0}}, \tag{40}$$

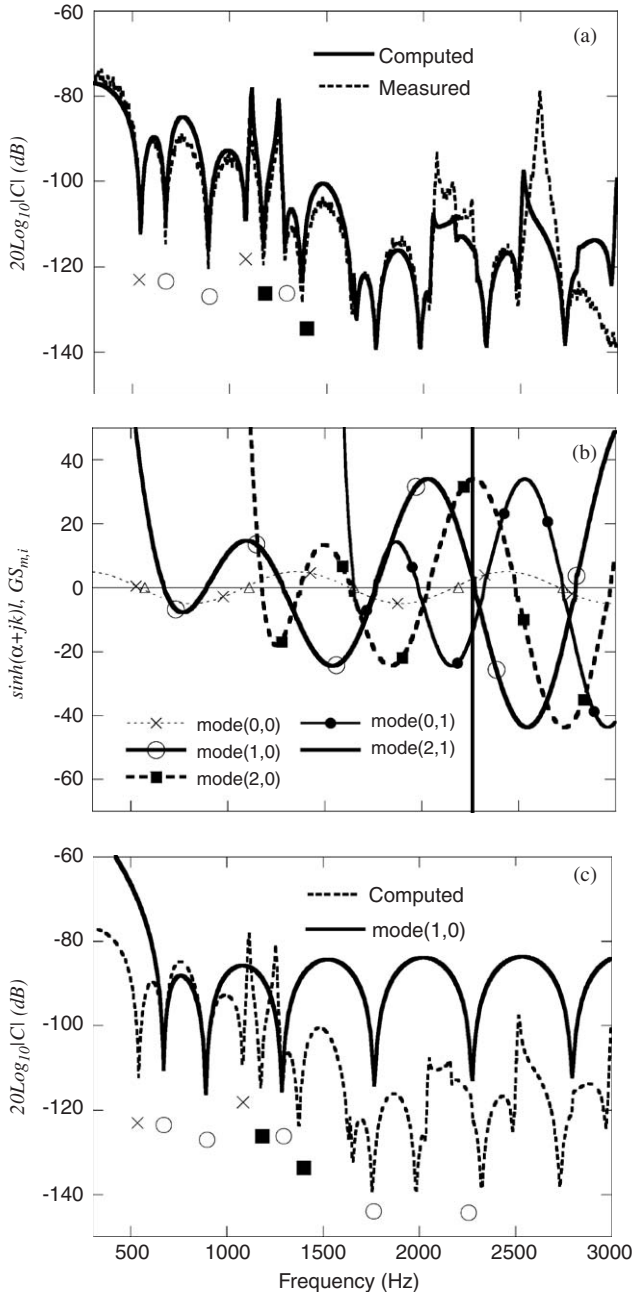

Fig. 3. The generation mechanism of parameter C: (a) Computed and measured results, (b) resonance mechanism, and (c) level of (1,0) mode.

where r_0 is set by the average of major and minor semi-axis of elliptical chamber. The acoustic impedance of perforated pipe is given by [8]

$$Z_{\text{pipe}} = \frac{\rho c}{S_f \sigma}(6 \times 10^{-3} + \mathrm{j}k(t + 0.75d_h)), \tag{41}$$

where S_f is the surface area, σ is the porosity and the equivalent thickness of the holes is $t + 0.75d_h$ in which d_h is a hole diameter.

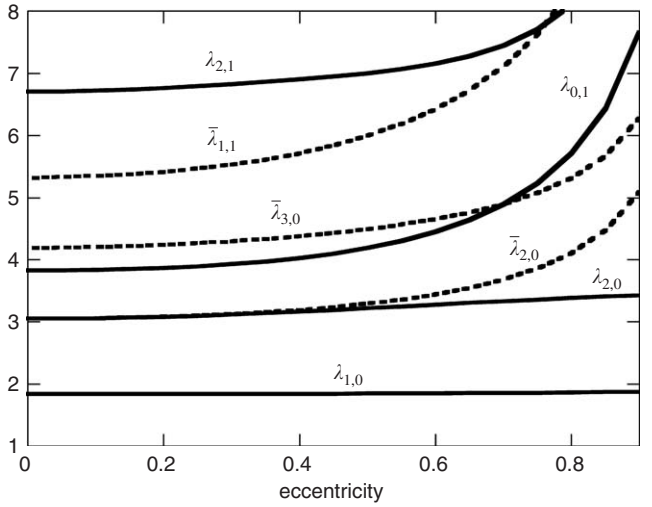

Fig. 4. Relationship between eccentricity and of higher-order modes.

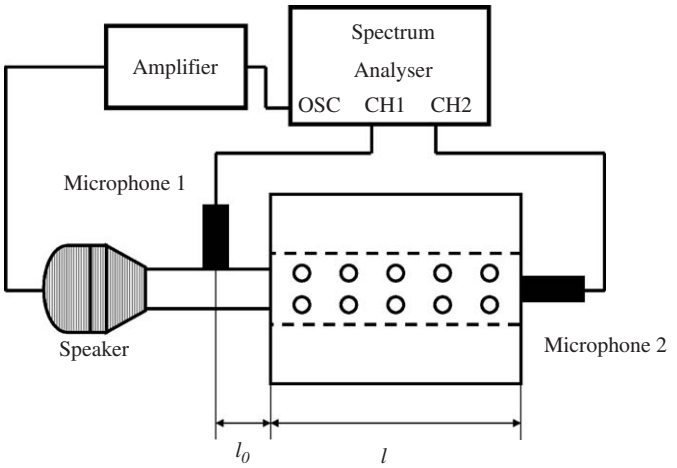

Fig. 5. Block diagram of the experimental apparatus.

In order to examine the correctness of the predicted theoretical, the measurement of parameter C was performed. A block diagram of the whole experimental apparatus [9] is shown in Fig. 5. Two microphones were located at both sides of the chamber to measure the sound pressures P_A and P_B. The dimensions of the chamber considered in this work are $e_w = 0.6$, $a_w = 15\,\text{cm}$, $l = 35\,\text{cm}$. The perforated pipe had a wall thickness of 0.5 mm. It was drilled with 0.6 cm diameter holes and 1.5 cm pitch so that the porosity, the ratio of the total hole areas to the pipe surface area, is 10%. Eccentricity $e_p = 0.85$ was selected to satisfy the condition $e_p a_p = e_w a_w$, and this means both the chamber and perforated pipe have the same foci.

From Fig. 5, the relationship between P_A and P_B is given by

$$\begin{pmatrix} P_A \\ U_A \end{pmatrix} = \begin{pmatrix} \cos kl_0 & \mathrm{j}Z_0 \sin kl_0 \\ \mathrm{j}\frac{1}{Z_0} \sin kl_0 & \cos kl_0 \end{pmatrix} \begin{pmatrix} A & B \\ C & D \end{pmatrix} \begin{pmatrix} P_A \\ U_B \end{pmatrix}, \tag{42}$$

where the first term represents the four-pole parameters of the input pipe which has length l_0 and the second represents our model chamber. Symbols U_A, U_B and Z_0 represent volume velocity and acoustic impedance of inlet pipe, respectively. By installing the microphone 2 on the output piston, U_B will become zero; thus,

Eq. (42) can be written as

$$P_A = (\cos kl_0\, A + Z_0 \sin kl_0 C)P_B. \tag{43}$$

Furthermore, since the first term can be disregarded as compared to the second term, Eq. (43) can be written in terms of dB as follows:

$$20\log_{10}|C| = 20\log_{10}|P_A/P_B| - 20\log_{10}|Z_0 \sin kl_0|. \tag{44}$$

This means parameter C can be found by subtracting the acoustic characteristic of inlet pipe $Z_0 \sin kl_0$ from the measured sound pressures P_A and P_B. Note that Eq. (44) corresponds to our theoretical Eq. (36).

Measured results are shown by the dotted line in Fig. 3(a). Except for the difference in the level caused by the attenuation factor α used in the calculation, the agreement observed between the measurement and the analytical prediction is acceptable. There are also some differences in the levels for a frequencies above 2250 Hz caused by the effect of (2,1) mode which is not considered in our calculation.

4. A special case

The four-pole parameters are derived from Eqs. (32) to (35). From these equations we can easily obtain the four-pole parameters. In case the perforated pipe is not attached by letting $\ddot{Z}_{m,i}$, the term related to acoustic impedance of perforated pipe defined by Eq. (A.24), tends to zero. We now have

$$A = \cosh(\alpha + \mathrm{j}k)l + \frac{\dot{\Sigma}\, GT_{m,i}\overline{Q^{0,0}_{m,i}}}{\dot{\Sigma}\, GS_{m,i}\overline{Q^{0,l}_{m,i}}}, \tag{45}$$

$$B = Z_w \sinh(\alpha + \mathrm{j}k)l + \mathrm{j}(k - \mathrm{j}\alpha)Z_w \dot{\Sigma}\, GS_{m,i} \times \left(\frac{GT^2_{m,i}\overline{Q^{0,0}_{m,i}}\,\overline{Q^{l,l}_{m,i}}}{GS^2_{m,i}\overline{Q^{0,l}_{m,i}}} - 1\right)\overline{Q^{0,l}_{m,i}}, \tag{46}$$

$$C = 1 \Big/ \left(\frac{Z_w}{\sinh(\alpha + \mathrm{j}k)l} + (\mathrm{j}k + \alpha)Z_w \dot{\Sigma}\, GS_{m,i}\overline{Q^{0,l}_{m,i}}\right), \tag{47}$$

$$D = \cosh(\alpha + \mathrm{j}k)l + \frac{\dot{\Sigma}\, GT_{m,i}\overline{Q^{l,l}_{m,i}}}{\dot{\Sigma}\, GS_{m,i}\overline{Q^{0,l}_{m,i}}}, \tag{48}$$

in which $GS_{m,i}$ and $GT_{m,i}$ become

$$GS_{m,i} = \frac{1}{\mu_{m,i}\sinh\mu_{m,i}l}, \tag{49}$$

$$GT_{m,i} = \frac{1}{\mu_{m,i}\tanh\mu_{m,i}l}. \tag{50}$$

In this case, only the even modes of the ($2m$, i) order may propagate due to symmetry. So the higher-order modes are generated in order of mode (2,0), (0,1) and so on. Fig. 6 shows parameter C in the cases with and without perforated pipe. It is clearly recognized that by the presence of mode (1,0), the one-dimensional frequency range when using a perforated pipe is narrower than without one.

When the cross section of the chamber and perforated pipe are circular, the four-pole parameters can be easily derived from our results by letting the eccentricity of their section tend to zero. The difference between this case and the elliptical case is $\overline{Q^{\mu,v}_{m,i}}$ in Eqs. (32)–(35). When the eccentricity tends to zero, namely, $\xi \to \infty$, $q \to 0$ the relations $ce_m(\eta,s) \to \cos m\eta$, $se_m(\eta,s) \to \sin m\eta$, $Ce_m(\xi,s) \to J_m(\lambda r/r_w)$, $se_{m+1}(\xi,s) \to J_{m+1}(\lambda r/r_w)$

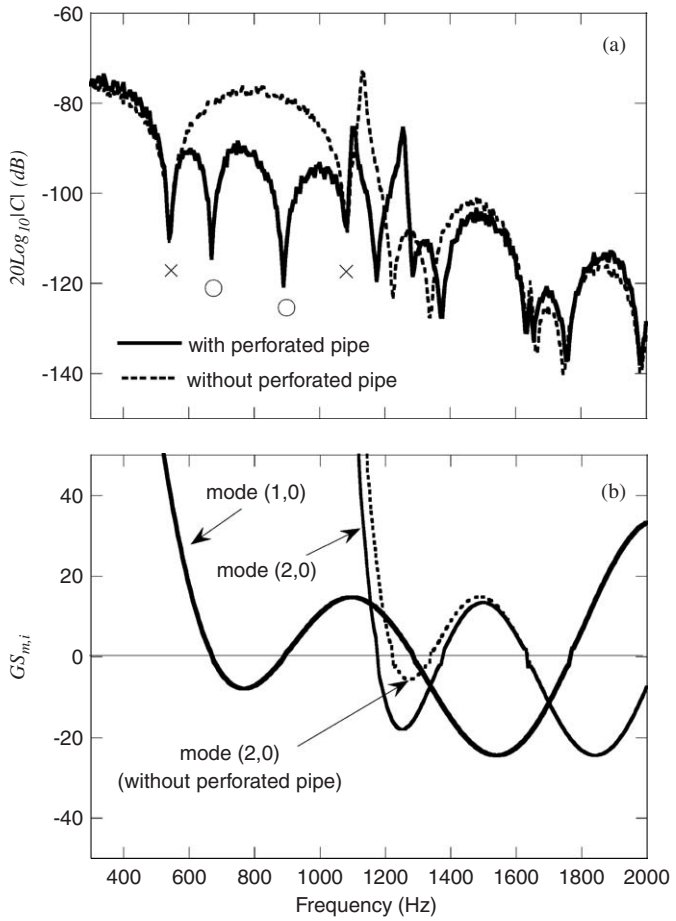

Fig. 6. Parameter C in case of with and without perforated pipe: (a) measured results, and (b) calculated results from Eq. (13) (with perforated pipe) and Eq. (46) (without perforated pipe).

are obtained [6]. Applying these relations and substituting into Eqs. (29)–(32) we have the four-pole parameters:

$$A = \cosh(\alpha + \mathrm{j}k)l + \frac{\dot{\Sigma}\, GT_{m,i}\overline{Q^{0,0}_{m,i}}(1+\ddot{Z}_{m,i})}{\dot{\Sigma}\, GS_{m,i}\overline{Q^{0,l}_{m,i}}(1+\ddot{Z}_{m,i})}, \tag{51}$$

$$B = Z_w \sinh(\alpha + \mathrm{j}k)l + \mathrm{j}(k\mathrm{j} - \alpha)Z_w \dot{\Sigma}\, GS_{m,i}\left(\frac{GT^2_{m,i}\overline{Q^{0,0}_{m,i}}\,\overline{Q^{l,l}_{m,i}}}{GS^2_{m,i}\overline{Q^{0,l}_{m,i}}} - 1\right)\overline{Q^{0,l}_{m,i}}(1+\ddot{Z}_{m,i}), \tag{52}$$

$$C = 1\Big/\left(\frac{Z_w}{\sinh(\alpha + \mathrm{j}k)l} + (\mathrm{j}k + \alpha)Z_w \dot{\Sigma}\, GS_{m,i}\overline{Q^{0,l}_{m,i}}(1+\ddot{Z}_{m,i})\right), \tag{53}$$

$$D = \cosh(\alpha + \mathrm{j}k)l + \frac{\dot{\Sigma}\, GT_{m,i}\overline{Q^{l,l}_{m,i}}}{\dot{\Sigma}\, GS_{m,i}\overline{Q^{0,l}_{m,i}}}, \tag{54}$$

in which

$$\overline{Q_{m,i}^{u,v}} = \frac{r_w}{r_u r_v} \frac{\int_0^{r_u}\int_0^{2\pi} rJ_m(\lambda_{m,i}(r/r_w))\cos\, m\theta\, \mathrm{d}r\, \mathrm{d}\theta}{\int_0^{r_w} rJ_m^2(\lambda_{m,i}(r/r_w))\mathrm{d}r \times \int_0^{r_v}\int_0^{2\pi} rJ_m(\lambda_{m,i}(r/r_w))\cos\, m\theta\, \mathrm{d}r\, \mathrm{d}\theta}, \tag{55}$$

$$c_1 = J_m(\lambda_{m,i} r_p r_w)/J'_m(\lambda_{m,i} r_p r_w), \tag{56}$$

$$c_2 = J_{m+1}(\lambda_{m,i} r_p r_w)/J'_{m+1}(\lambda_{m,i} r_p r_w), \tag{57}$$

$$\Gamma_{m,i} = \frac{1}{(c_1 - c_2)}\left(1 - \frac{J'_m(\lambda^r_{m,i} r_w)J_{m+1}(\lambda^r_{m,i} r_w)}{J_m(\lambda^r_{m,i} r_w)J'_{m+1}(\lambda^r_{m,i} r_w)}\right), \tag{58}$$

$J_m(x)$ represents the Bessel functions of mth order, r_p and r_w are the radius of perforated pipe and the chamber, respectively.

5. Conclusion

The derivation of the four-pole parameters for the elliptical chamber having a perforated pipe has been presented by solving the equations, considering the higher-order mode effects. The four-pole parameters are given by Eqs. (32)–(35). Based on the results obtained, the cause and mechanism of resonance frequencies of parameter C is discussed in detail. A good correlation between the prediction and experiment of parameter C is observed. Our results can be applied to a chamber without a perforated pipe and both chamber and perforated pipe in circular section. Those four-pole parameters are given by Eqs. (45)–(47) and Eqs. (51)–(54), respectively.

Appendix A

In order to find ϕ_{in} and ϕ_{out} from Eqs. (5) to (9), let ϕ^a_{in} and ϕ^a_{out} be solutions of Eqs. (3) and (4) obtained for the following boundary conditions:

$$\text{[1a]} \quad \text{at} \quad z = 0, \;\; V_z = -\partial\phi^a_{\mathrm{in}}/\partial z = V_0 F_0(\xi, \eta), \tag{A.1}$$

$$\text{[2a]} \quad \text{at} \quad z = 1, \;\; V_z = -\partial\phi^a_{\mathrm{in}}/\partial z = 0, \tag{A.2}$$

$$\text{[3a]} \quad \text{at} \quad \xi = \xi_w, \;\; V_\xi = -\partial\phi^a_{\mathrm{out}}/\partial\xi = 0, \tag{A.3}$$

$$\text{[4a]} \quad \text{at} \quad z = l, \;\; V_z = -\partial\phi^a_{\mathrm{out}}/\partial z = 0, \tag{A.4}$$

$$\text{[5a]} \quad \text{at} \quad \xi = \xi_p, \;\; \phi^a_{\mathrm{in}} - \phi^a_{\mathrm{out}} = \frac{Z_{\mathrm{pipe}}}{\mathrm{j}k\rho c}\frac{\partial\phi^a_{\mathrm{out}}}{\partial\xi}, \tag{A.5}$$

$$\text{[6a]} \quad \text{at} \quad \xi = \xi_p, \;\; \partial\phi^a_{\mathrm{in}}/\partial\xi = \partial\phi^a_{\mathrm{out}}/\partial\xi, \tag{A.6}$$

and let ϕ^b_{in} and ϕ^b_{out} be solutions of Eqs. (3) and (4) obtained for the following boundary conditions:

$$\text{[1b]} \quad \text{at} \quad z = 0, \quad V_z = -\partial\phi^b_{\mathrm{in}}/\partial z = 0, \tag{A.7}$$

$$\text{[2b]} \quad \text{at} \quad z = l, \quad V_z = -\partial\phi^b_{\mathrm{in}}/\partial z = V_l F_l(\xi, \eta), \tag{A.8}$$

$$\text{[3a]} \quad \text{at} \quad \xi = \xi_w, \quad V_\xi = -\partial\phi^b_{\mathrm{out}}/\partial\xi = 0, \tag{A.9}$$

$$\text{[4b]} \quad \text{at} \quad z = 0, \quad V_z = -\partial\phi^b_{\mathrm{out}}/\partial z = 0, \tag{A.10}$$

$$\text{[5b]} \quad \text{at} \quad \xi = \xi_p, \quad \phi^b_{\mathrm{in}} - \phi^b_{\mathrm{out}} = \frac{Z_{\mathrm{hole}}}{jk\rho c}\frac{\partial\phi^b_{\mathrm{out}}}{\partial\xi}, \tag{A.11}$$

$$[6b] \quad \text{at} \quad \xi = \xi_p, \quad \partial\phi_{\text{in}}^b - \partial\xi = \partial\phi_{\text{out}}^b/\partial\xi. \tag{A.12}$$

Then ϕ_{in} and ϕ_{out} can be obtained as $\phi_{\text{in}} = \phi_{\text{in}}^a + \phi_{\text{in}}^b$ and $\phi_{\text{out}} = \phi_{\text{out}}^a + \phi_{\text{ut}}^b$, respectively.

At first, ϕ_{in} can be derived by the following procedure. From Eq. (A.2) we have

$$B_i = A_i \exp(2\mu l). \tag{A.13}$$

Substituting Eq. (A.13) into Eq. (3), we have

$$\phi_{\text{in}}^a = \sum_{m=0}^{\infty} A_i f(z,\mu) Ce_m(\xi,s) ce_m(\eta,s), \tag{A.14}$$

where

$$f(z,\mu) = \exp(\mu z) + \exp(2\mu l)\exp(-\mu z). \tag{A.15}$$

Similarly, find B_0 from Eq. (A.4) and substituting into Eq. (4) we obtain

$$\phi_{\text{out}} = \sum_{m=0}^{\infty} C_m^0 f(z,\mu) Ce_m(\xi,s) ce_m(\eta,s) + \sum_{m=0}^{\infty} S_{m+1}^0 f(z,\mu) Se_{m+1}(\xi,s) se_{m+1}(\eta,s) \tag{A.16}$$

and from Eq. (A.3) we have

$$\sum_{m=0}^{\infty} C_m^0 f(z,\mu) Ce'_m(\xi_w,s) ce_m(\eta,s) + \sum_{m=0}^{\infty} S_{m+1}^0 f(z,\mu) Se'_{m+1}(\xi_w,s) se_{m+1}(\eta,s) = 0. \tag{A.17}$$

To make Eq. (A.17) always zero, it is necessary that

$$Ce'_m(\xi_w,s) = \left.\frac{\partial Ce_m(\xi,s)}{\partial\xi}\right|_{\xi=\xi_w} = 0 \tag{A.18}$$

and

$$Se'_m(\xi_w,s) = \left.\frac{\partial Se_{m+1}(\xi,s)}{\partial\xi}\right|_{\xi=\xi_w} = 0. \tag{A.19}$$

Letting the positive roots of Eqs. (A.18) and (A.19) be $s_{m,i}$ and $\overline{s_{m+1,i}}(i = 0, 1, 2, \ldots)$, respectively, and letting μ correspond to $s_{m,i}$ and $\overline{s_{m+1,i}}$ to be $\mu_{m,i}$ and $\overline{\mu_{m+1,i}}\phi_{\text{in}}^a$, then ϕ_{out}^a can be obtained as

$$\phi_{\text{in}}^a = \sum_{m=0}^{\infty}\sum_{i=0}^{\infty} A_{m,i} f(z,\mu_{m,i}) Ce_m(\xi,s_{m,i}) ce_m(\eta,s_{m,i}), \tag{A.20}$$

$$\phi_{\text{out}}^a = \sum_{m=0}^{\infty}\sum_{i=0}^{\infty} C_{m,i} f(z,\mu_{m,i}) Ce_m(\xi,s_{m,i}) ce_m(\eta,s_{m,i}) + \sum_{m=0}^{\infty}\sum_{i=0}^{\infty}\left(S_{m+1,i} f(z,\overline{\mu_{m+1,i}}) Se_{m+1}(\xi,\overline{s_{m+1,i}}) se_{m+1}(\eta,\overline{s_{m+1,i}})\right). \tag{A.21}$$

Next, derive $A_{m,i}$ from Eq. (A.5) and considering Eq. (A.6) we have

$$C_{m,i} f'(z,\mu_{m,i}) Ce_m(\xi,s_{m,i}) ce_m(\eta,s_{m,i})\big|_{z=0} = -V_0 F_0(\xi,\eta). \tag{A.22}$$

By multiplying both sides of Eq. (A.22) by $Ce_m(\xi,s_{m,i})ce_m(\eta,s_{m,i})(\cosh 2\xi - \cos 2\eta)$ and integrating with respect to ξ from 0 to ξ_w and with respect to η from 0 to 2π, we can determine the constant $C_{m,i}$. Thus ϕ_{in}^a becomes

$$\phi_{\text{in}}^a = \sum_{m=0}^{\infty}\sum_{i=0}^{\infty} \frac{V_0}{\frac{\mu_{m,i}\sinh\mu_{m,i}l}{\cosh\mu_{m,i}(1-z)} + Z_{m,i}\frac{\overline{\mu_{m+1,i}}\sinh\overline{\mu_{m+1,i}}l}{\cosh\overline{\mu_{m+1,i}}(1-z)}} H_{m,i}^0 (1+\ddot{Z}_{m,i}) \Theta_m(\xi,\eta,s_{m,i}), \tag{A.23}$$

where

$$\ddot{Z}_{m,i} = \frac{Z_{pn}(c_2 + Z_{pn})}{(c_1 + Z_{pn})(c_1 - c_2 - Z_{pn})}, \tag{A.24}$$

$$Z_{pn} = \frac{Z_{\text{pipe}}}{\mathrm{j}k\rho c}, \tag{A.25}$$

$$c_1 = \frac{Ce_m(\xi_p, s_{m,i})}{Ce'_m(\xi_p, s_{m,i})}, \tag{A.26}$$

$$c_2 = \frac{Se_{m+1}(\xi_p, \overline{s_{m+1,i}})}{Se'_{m+1}(\xi_p, \overline{s_{m+1,i}})}, \tag{A.27}$$

$$\Theta_m = (\xi, \eta, s_{m,i}) = Ce_m(\xi, s_{m,i}) ce_m(\eta, s_{m,i}), \tag{A.28}$$

$$g(\xi, \eta) = \cosh 2\xi - \cos 2\eta, \tag{A.29}$$

$$H^u_{m,i} = \int_0^{\xi_u} \int_0^{2\pi} \Theta_m(\xi, \eta, s_{m,i}) g(\xi, \eta) \mathrm{d}\xi \, \mathrm{d}\eta \Big/ \int_0^{\xi_u} \int_0^{2\pi} \Theta^2_m(\xi, \eta, s_{m,i}) g(\xi, \eta) \mathrm{d}\xi \, \mathrm{d}\eta. \tag{A.30}$$

Similarly, by using Eqs. (A.7)–(A.12), ϕ^b_{in} can be obtained:

$$\phi^b_{\text{in}} = \sum_{m=0}^{\infty} \sum_{i=0}^{\infty} \frac{V_l}{\frac{\mu_{m,i} \sinh \mu_{m,i} l}{\cosh \mu_{m,i} z} + \ddot{Z}_{m,i} \frac{\bar{\mu}_{m+1,i} \sinh \overline{\mu_{m+1,i} l}}{\cosh \overline{\mu_{m+1,i} z}}} H^l_{m,i} (1 + \ddot{Z}_{m,i}) \Theta_m(\xi, \eta, s_{m,i}), \tag{A.31}$$

where $H_{m,i}{}^{l}$ is defined by Eq. (A.29) in which ξ_0 is replaced by ξ_l. Thus, from Eqs. (A.23) and (A.31), we obtain

$$\phi_{\text{in}} = \phi^a_{\text{in}} + \phi^b_{\text{in}} = \sum_{m=0}^{\infty} \sum_{i=0}^{\infty} \left(\frac{H^0_{m,i} V_0}{\frac{\mu_{m,i} \sinh \mu_{m,i} l}{\cosh \mu_{m,i}(1-z)} + \ddot{Z}_{m,i} \frac{\overline{\mu_{m+1,i}} \sinh \overline{\mu_{m+1,i} l}}{\cosh \overline{\mu_{m+1,i}}(1-z)}} - \frac{H^l_{m,i} V_l}{\frac{\mu_{m,i} \sinh \mu_{m,i} l}{\cosh \mu_{m,i} z} + \ddot{Z}_{m,i} \frac{\overline{\mu_{m+1,i}} \sinh \overline{\mu_{m+1,i} l}}{\cosh \overline{\mu_{m+1,i} z}}} \right) (1 + \ddot{Z}_{m,i}) \Theta_m(\xi, \eta, s_{m,i}). \tag{A.32}$$

References

[1] J.W. Sullivan, M.J. Crocker, Analysis of concentric tube resonators having unpartitioned cavities, *Journal Acoustic Society of America* 64 (1978) 207–215.

[2] J.W. Sullivan, A method for modeling perforated tube muffler components. 1. Theory, *Journal Acoustic Society of America* 66 (1979) 772–788.

[3] K.S. Peat, A numerical decoupling analysis of perforated pipe silencer elements, *Journal of Sound and Vibration* 123 (1988) 199–212.

[4] H. Luo, C.C. Tse, Y.N. Chen, Modeling and applications of partially perforated intruding tube mufflers, *Applied Acoustics* 44 (1995) 99–116.

[5] C.N. Wang, A numerical scheme for the analysis of perforated introding tube muffler components, *Applied Acoustic* 44 (1995) 275–286.

[6] N.W. McLachlan, *Theory and Application of Mathieu Functions*, Clarendon Press, Oxford, 1947.

[7] ASTM E1055-86. Standard test method for impedance and absorption of acoustical materials using a tube, Two microphones, and Digital frequency analysis system. American Society for Testing Materials, Philadelphia, PA, 1986.

[8] M.L. Munjal, *Acoustics of Ducts and Mufflers*, Wiley, New York, 1987.

[9] N.M. Cuong, J. Okda, On fitting position of inlet and outlet pipes to elliptic cylindrical muffler chambers, *Journal Acoustic Society of Japan (E)* 2 (1981) 71–78.